MORTAR FINITE ELEMENT METHOD FOR SOLVING CELLS RESPONSE TO APPLIED ELECTRIC FIELD

Cesar A Conopoima

Bernardo M Rocha

Iury A da Igreja

Rodrigo W dos Santos

cesar.conopoima@gmail.com

bernardomartinsrocha@ice.ufjf.br

iuryigreja@ice.ufjf.br

rodrigo.weber@ufjf.edu.br

Universidade Federal de Juiz de Fora

CEP 36036-330 - Juiz de Fora - MG - Brazil

Abstract. *In this work we investigate the response of passive and active biological cell to an applied electrical field. This phenomenon is a two-stage process where cell polarization occurs at a time scale of microseconds, and change of physiological state of the cells occurs at the time scale of milliseconds. This problem is solved using a Mortar Finite Element Method (MFEM) that is characterized by the introduction of an additional variable, known as Lagrange multiplier. This additional variable allows to decouple the boundary value problem that describes the conservation of electrical flux from the non-linear initial value system related to the response of active cells. This two problems are solved sequentially, within the time integration scheme. The proposed method allows to solve arbitrary cells distribution in tissues and complex ion-channel dynamics at the membrane. In order to validate the presented methodology, numerical results are compared with exact solutions of isolated circular cells in an applied electrical field. Finally, to demonstrate the robustness of the method, applied electrical field in clusters of cells and arbitrary cell geometry problems are solved.*

Keywords: *Mortar finite element method, Lagrange multiplier, Cell polarization, Active cell response.*

1 INTRODUCTION

The response of a single cell and cluster of cells to external applied electrical field is important for the understanding of techniques such as cell electroporation (Orlowski & Mir, 1993, Chen *et al.*, 2006), which is the transient permeabilization of the plasma membrane by means of short and intense electric pulse. This technique has broad application in the biological and medical community for instance for the local treatment of cancer. Since the cells cytosol becomes accessible to the external medium, DNA and molecules transference into the cell are possible, direct drug supply is also possible without compromising cell function (Orlowski & Mir, 1993, Chen *et al.*, 2006). Moreover, it is not clear if cell electroporation does play an important role in cardiac defibrillation, therefore this is also a relevant topic in the research field of cardiac electrophysiology (ASHIHARA *et al.*, 2001, KRASSOWSKA, 1995, Nikolski & Efimov, 2005).

Properly studying extracellular potential distribution in cluster of cells of arbitrary geometry is important to understand the influence of applied electrical field in neurons activity (Agudelo-Toro & Neef, 2013). Particular solutions to describe the passive response of cells to applied field are available for isolated cells of simple circular and ellipsoidal geometry (Krassowska & Neu, 1994, Gimsa & Wachner, 2001). Although exact solutions for spherical cells in non uniform electric field exists (Valič *et al.*, 2003, Lee & Grill, 2005), a general tool to numerically investigate cells electroporation and extracellular potential distribution is of interest. In this sense, the numerical study of the passive and active response of isolated cells to external field has been made in (Ying & Henriquez, 2007, Pucihar *et al.*, 2009). Furthermore the influence of cells arrangement, orientation and cells packing in the presence of external electrical applied field has also been investigated in (Susil *et al.*, 1998, Ying *et al.*, 2006, Ying & Henriquez, 2007, Agudelo-Toro & Neef, 2013).

The response of biological cells to applied electrical field is a two stage process (Krassowska & Neu, 1994, Ying & Henriquez, 2007): the first stage takes place at the time scale of microseconds, where the capacitive current is dominant and the cell behaves like a dipole; in the second stage actual physiological changes due to the complex dynamic of ion currents on the cell membrane takes place, which is triggered if the transmembranic current on the first stage is sufficiently high to unchain action potential on the cell (Keener & Sneyd, 2010). Moreover the active response of the cell will also be influenced by the distribution and packing of the cells (Ying *et al.*, 2006, Agudelo-Toro & Neef, 2013), because of the complex interactions in cells arrangements, possible irregular cells geometries and the lack of exact solutions in those cases, the study of the distribution of electric potential and of the action potential in non-idealized systems of multiple cells can only be studied by numerical methods.

In the context of the Finite Element Methods (FEM), simulations of cells electroporation in tumours (Šemrov & Miklavčič, 2000), non regular cell geometry (Pucihar *et al.*, 2009) and spherical cell arrangements (Susil *et al.*, 1998) have been investigated. In (Ying *et al.*, 2006, Agudelo-Toro & Neef, 2013) a Hybrid Finite Element Method (HFEM) is used to investigate the passive and active cell response to external applied electrical fields. With this method the boundary value problem of electric current conservation and the initial value problem of active cell response are decoupled and solved in alternate form in each time step. The HFEM is based on the hypothesis that cell membrane is a zero thickness domain i.e, an interface that separates two non overlapping domains (Ying & Henriquez, 2007), one describing the intra and other the

extracellular domain. On the membrane a compatibility conditions must be satisfied, on the hybrid finite element method the interface condition is satisfied by the inclusion of a Lagrange multiplier.

The proper treatment of interface conditions in finite element methods (Ciarlet *et al.*, 1975, Raviart *et al.*, 1998), requires the imposition of continuity of the solution on the interface through Lagrange multipliers, as proposed by Raviart-Thomas in the known primal hybrid formulation (Raviart & Thomas, 1977). This approach allows to have non-conforming domain discretizations with optimal convergence order for both the primal and Lagrange multiplier variables (Bernardi *et al.*, 1993, Belgacem, 1999).

In order to satisfy the compatibility condition between spaces (LBB inf-sup condition) in the primal hybrid formulation, the Lagrange multiplier must be properly defined. The formal treatment and analysis of this method are defined in the literature as Mortar Finite Element Method (Bernardi *et al.*, 1993, Belgacem, 1999, Wohlmuth, 2000, Lamichhane, 2006); and has the main advantage of allowing to solve interface problems with non-matching domain triangulations. The linear system associated with the discrete version of this formulation has a saddle point problem structure and in general is difficult to numerically solve (Benzi *et al.*, 2005).

1.1 Objective

The aim of this work is to present a mortar finite element method based on a hybrid variational formulation, to numerically investigate the interface problem with complex dynamics of the passive and active response of a cell and cluster of cells to an applied electric field.

2 CONSERVATION LAW OF ELECTRIC CURRENT

The electric field in a biological tissue resulting from the application of a direct current can be considered quasi-stationary (Plonsey & Heppner, 1967), this means that its distribution is described by equations of the steady electric current in a volume conductor. The relation of electric current to voltage and resistance is described by Ohm's law. The electric current density $\mathbf{J}[\mathrm{A}\cdot\mathrm{cm}^{-3}]$ is defined by the point form of the Ohm's law $\mathbf{J} = \boldsymbol{\kappa}\cdot\mathbf{E}$, where $\mathbf{E}[\mathrm{V}\cdot\mathrm{cm}^{-1}]$ is the electric vector field. For a conservative electric field we can write the electric field $\mathbf{E}$ in function of the electric potential $u[\mathrm{V}]$,

$$\mathbf{E} = -\nabla u, \tag{1}$$

by continuity of current density, the Kirchoff's law can be written in differential form as $\mathrm{div}(\mathbf{J}) = \rho_s$, where $\rho_s[\mathrm{A}\cdot\mathrm{cm}^{-3}]$ is an applied source current. Now with the Ohm's law applied to a conservative electric field, we can write the Kirchoff's law in function of the electric potential u,

$$-\mathrm{div}(\boldsymbol{\kappa}\nabla u) = \rho_s, \tag{2}$$

Eq. (2) is the Poisson's equation that describe the electric potential distribution in a resistive biological tissue with an applied source current. The Poisson's problem is defined on a domain $\Omega \subset \mathbb{R}^d$, where $d \in \{1, 2, 3\}$ with a Lipschitz boundary $\partial\Omega = \Gamma_D \cup \Gamma_N, \Gamma_D \cap \Gamma_N = \emptyset$.

$$
\begin{aligned}
-\text{div}(\boldsymbol{\kappa}\nabla u) &= \rho_s(\mathbf{x}), \quad \text{in } \Omega \\
u &= \hat{u}, \quad \text{on } \Gamma_D \\
\nabla u \cdot \mathbf{n} &= \rho_n, \quad \text{on } \Gamma_N
\end{aligned} \tag{3}
$$

$\hat{u}$ is the known scalar electric potential defined on the Dirichlet boundary portion Γ_D, and ρ_n is the applied current on the Neumann boundary portion of the domain Γ_N.

2.1 Conservation of electric current for a circular cell in a conductive suspension

Consider a circular cell of diameter d_c and conductivity $\boldsymbol{\kappa_i}$, in a bounded domain Ω_e with electrical conductivity $\boldsymbol{\kappa_e}$ subject to an applied electrical field $\mathbf{E}$ as depicted in figure 1. The Poisson's equation of electric current conservation (4) for the proposed system, is written as a function of the electric potential inside and outside the cell (u_i, u_e), that is

$$
\begin{aligned}
-\text{div}(\boldsymbol{\kappa_e}\nabla u_e) &= 0, \quad \text{in } \Omega_e, \\
-\text{div}(\boldsymbol{\kappa_i}\nabla u_i) &= 0, \quad \text{in } \Omega_i, \\
\boldsymbol{\kappa_i}\nabla u_i \cdot \mathbf{n} = -\boldsymbol{\kappa_e}\nabla u_e \cdot \mathbf{n} &= I_m, \quad \text{on } \Gamma, \\
u_e &= \hat{u}, \quad \text{on } \Gamma_D, \\
\nabla u_e \cdot \mathbf{n}_e &= 0, \quad \text{on } \Gamma_N
\end{aligned} \tag{4}
$$

with the additional interface condition defined on Γ that force continuity of electric flux through the cell membrane $-\boldsymbol{\kappa_i}\nabla u_i \cdot \mathbf{n} = -\boldsymbol{\kappa_e}\nabla u_e \cdot \mathbf{n} = I_m, \text{ on } \Gamma$.

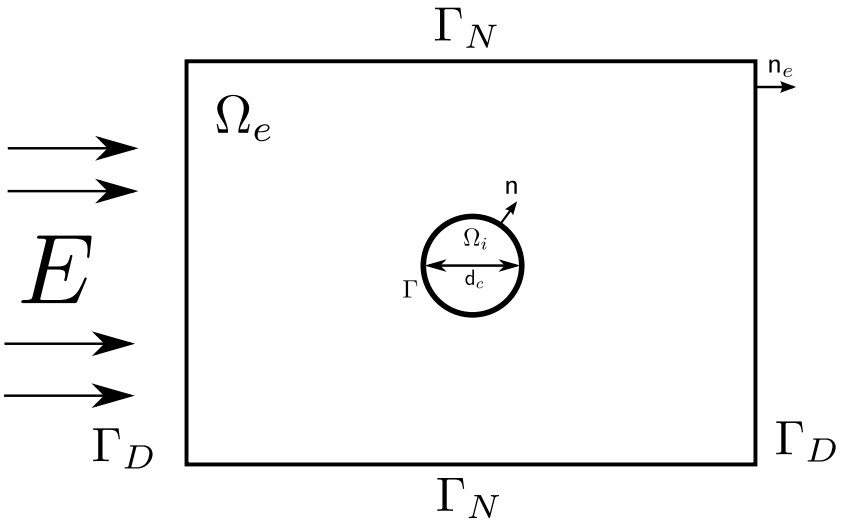

Figure 1: A circular cell in a conductive medium

In Eq. 4 Γ denotes the cell membrane, $\mathbf{n}$ is the unitary normal vector pointing outside of Γ and $I_m[\text{A} \cdot \text{cm}^{-2}]$ is the transmembranic current which has two components: a capacitive and a resistive current, both depending on the transmembranic potential defined by,

$$
V_m = u_i - u_e, \quad \text{on } \Gamma. \tag{5}
$$

The transmembranic current can be written as the contribution of two currents: the capacitive and the resistive or ionic current given by,

$$I_m = C_m \frac{\partial V_m}{\partial t} + I_{ion}(V_m, \mathbf{q}), \quad \text{on } \Gamma. \tag{6}$$

The capacitive current is a consequence of the electric isolation property of the cell membrane. The cell polarization due to capacitive currents occurs at the time scale of microseconds, whereas for the active response of the cell membrane, the resistive or ionic current acts at time scale of milliseconds and is determined by the complex dynamics of the sodium, potassium and other important ionic currents, described for instance by the non-linear equations of the Hodgkin Huxley model (Hodgkin & Huxley, 1952, Keener & Sneyd, 2010), represented by the state variable $\mathbf{q}$ in Eq. (6).

3 VARIATIONAL FORMULATION OF THE CONSERVATION PROBLEM

Given the electric current conservation problem of the unicellular system in figure 1, for the sake of simplicity, let $\boldsymbol{\kappa_i} = \boldsymbol{\kappa_e}$ to be unitary second order tensor of the electric conductivity inside and outside the cell, the it is possible to rewrite the system (4) as,

$$\begin{aligned} -\Delta u_e &= 0, \quad \text{in } \Omega_e, \\ -\Delta u_i &= 0, \quad \text{in } \Omega_i, \\ \nabla u_i \cdot \mathbf{n} = -\nabla u_e \cdot \mathbf{n} &= I_m, \quad \text{on } \Gamma, \\ u_e &= \hat{u}, \quad \text{on } \Gamma_D, \\ \nabla u_e \cdot \mathbf{n}_e &= 0, \quad \text{on } \Gamma_N \end{aligned} \tag{7}$$

The variational formulation of problem (7), is written to reduce the required regularity of the candidate solution: find $u \in \mathcal{X}$ such that,

$$\begin{aligned} \int_\Omega \nabla u \cdot \nabla v dx - \int_{\partial\Omega} \nabla u \cdot \mathbf{n}_e v ds = 0, &\quad \text{in } \Omega \ \forall v \in \mathcal{X} \\ [u]|_\Gamma = g, &\quad \text{on } \Gamma \\ u_e = \hat{u}, &\quad \text{on } \Gamma_D \\ \nabla u_e \cdot \mathbf{n}_e = 0, &\quad \text{on } \Gamma_N \end{aligned} \tag{8}$$

where $\Omega = \Omega_i \cup \Omega_e$, $\Gamma = \Omega_i \cap \Omega_e$, $u = (u_i, u_e)$, $v = (v_i, v_e)$, $\hat{u}$ is the electric potential applied on Γ_D, $[u] = u_i|_\Gamma - u_e|_\Gamma$ is the scalar jump of electric potential on the membrane, and $\mathcal{X}$ is the constrained space of variations,

$$\mathcal{X} = \Big\{ v \in L^2(\Omega), (v_i, v_e) \in (H^1 \times H^1) : [v]|_\Gamma = 0, \ v_e|_{\Gamma_D} = 0 \Big\} \tag{9}$$

note that on the interface Γ the test function v on each domain must satisfy the constrain $[v] = 0$. The associated unconstrained product space of variations is denoted as

$$\tilde{\mathcal{X}} = \Big\{ v \in L^2(\Omega), (v_i, v_e) \in (H^1 \times H^1), \ v_e|_{\Gamma_D} = 0 \Big\}. \tag{10}$$

As proposed by Raviart-Thomas (Raviart & Thomas, 1977), an additional Hilbert space defined on Γ is included to impose the interface condition of the primal variable in a weak form via the use of a Lagrange multiplier. With this technique the constraint over v on the space $\mathcal{X}$ is also naturally relaxed and thus the primal hybrid variational formulation is: find $(u, \lambda) \in (\tilde{\mathcal{X}} \times \mathcal{M})$ such that,

$$\int_\Omega \nabla u \cdot \nabla v dx - \int_{\partial\Omega} \nabla u \cdot \mathbf{n}_e v ds + \int_\Gamma \mu([u] - g) ds + \int_\Gamma \lambda[v] ds = 0, \ \forall (v, \mu) \in \tilde{\mathcal{X}} \times \mathcal{M}, \tag{11}$$

$$u_e = \hat{u}, \quad \text{on } \Gamma_D,$$
$$\nabla u_e \cdot \mathbf{n}_e = 0, \quad \text{on } \Gamma_N$$

where λ is the Lagrange multiplier and μ are the admissible variation related to $\mathcal{M}$, which is the Hilbert space of the Lagrange multiplier. By duality argument, we note that $\mathcal{M} = H^{-\frac{1}{2}}(\Gamma)$, which is the dual space of $H^{\frac{1}{2}}(\Gamma)$ and therefore $\mu \in H^{-\frac{1}{2}}(\Gamma)$. The variational formulation (11) is known as a saddle point or as a min-max problem. By the natural Neumann boundary condition $\nabla u \cdot \mathbf{n}_e = 0$ on Γ_N, the second term of the formulation is neglected, and then the saddle point problem is: find $(u, \lambda) \in (\tilde{\mathcal{X}}, \mathcal{M})$ such that

$$\int_\Omega \nabla u \cdot \nabla v dx + \int_\Gamma \lambda[v] ds = 0, \quad \forall v \in \tilde{\mathcal{X}} \tag{12}$$

$$\int_\Gamma \mu([u] - g) ds = 0, \quad \forall \mu \in \mathcal{M}$$

$$u_e = \hat{u}, \quad \text{on } \Gamma_D.$$

Implicitly the following compatibility condition between spaces has been deduced, $I_m \equiv \lambda \equiv \nabla u_i \cdot \mathbf{n} \equiv -\nabla u_e \cdot \mathbf{n}$.

3.1 Time discretization for the transmembrane current

In this section the form of the general function g in the cell interface problem (12) is defined. As mentioned the transmembrane current can be decomposed in two contributions, a capacitive and a ionic current,

$$I_m = \frac{\partial V_m}{\partial t} + I_{ion}(V_m, q), \quad \text{on } \Gamma. \tag{13}$$

the capacitive current is consequence of the electric isolating property of the cell membrane, and for active cells as cardiac myocytes and neurons, the ionic current is driven by the complex interactions between the main ionic currents of sodium, potassium and others described by the Hodgkin-Huxley model. In order to include the transmembrane current dynamics described by Eq. (13) into the proposed variational formulation (12), we rewrite Eq. (13) as an initial value problem for the transmembranic potential V_m,

$$C_m \frac{\partial V_m}{\partial t} = I_m - I_{ion}(V_m, \mathbf{q}), \quad \text{on } \Gamma. \tag{14}$$

where **q** is a set of state variables following the dynamics of the ionic currents. Now by realizing that $V_m = [u] = g$ on Γ, we use an explicit time discretization for the initial value problem (14) and as in (Ying & Henriquez, 2007), use the follow staggered method to solve the coupled boundary value problem and initial value problem.

The first step of the proposed method is to solve the boundary value problem with a initial value of V_m^t.

$$\int_\Omega \nabla u \cdot \nabla v dx + \int_\Gamma \lambda[v] ds = 0, \quad \forall v \in \tilde{\mathcal{X}} \tag{15}$$
$$\int_\Gamma \mu[u] ds = \int_\Gamma \mu V_m^t ds, \quad \forall \mu \in \mathcal{M}$$
$$u_e = \hat{u}, \quad \text{on } \Gamma_D$$

with $I_m = \lambda$, solve the initial value problem (14) with a Forth Order Runge-Kutta method to obtain a new value of the transmembranic potential V_m^t at an incremented time $t + \delta t$. Finally, the method is closed repeating the first step with the new value of the transmembranic potential V_m^t.

4 THE MORTAR FINITE ELEMENT DISCRETIZATION

Now the finite element discretization of the variational formulation is proposed, from the definition of the Lagrange multiplier space, we note that the functions used to interpolate the discrete Lagrange multiplier λ are the same functions of $v|_e$ where e denotes an edge of the domain. For the classical Lagrangian polynomial space on triangular and quadrilateral finite elements in two dimensions, the interpolation function of the Lagrange multiplier match the classic hat functions with compact support in one dimension, see figure 3.

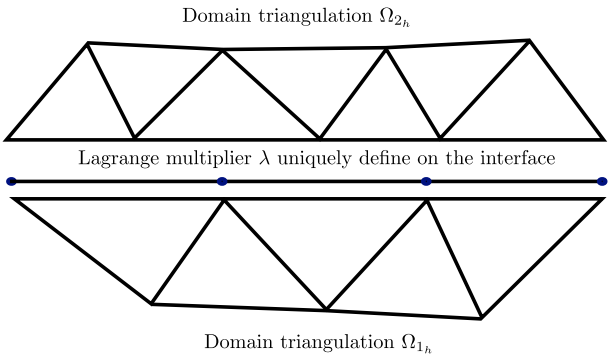

Figure 2: Triangulation in two non overlapping domains and Lagrange multiplier triangulation define on the non mortar side interface

Now the discrete mortar finite element problem is to find $(u_h, \lambda_h) \in \mathcal{X}_{n;h} \times \mathcal{M}_{n;h}$, such that u_h, λ_h are the unique discrete solutions to the saddle point problem 16.

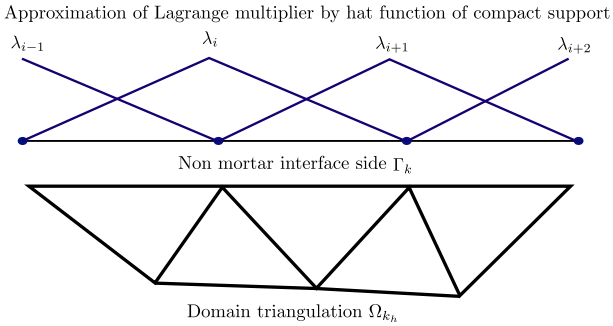

Figure 3: Triangulation of the Lagrange multiplier on the interface, and interpolation hat functions.

$$\begin{aligned} \int_\Omega \nabla u_h \cdot \nabla v_h dx + \int_\Gamma \lambda_h [v_h] ds = 0, \quad & \forall v_h \in \mathcal{X}_h \\ \int_\Gamma \mu_h [u_h] ds = \int_\Gamma \mu_h V_m^t ds, \quad & \forall \mu_h \in \mathcal{M}_h \\ u_e = \hat{u}, \quad \text{on } \Gamma_D & \end{aligned} \tag{16}$$

where the discrete spaces of variations $\mathcal{X}_h \subset \tilde{\mathcal{X}}$ is the product space of discrete Lagrange polynomial defined on each triangulated domain, and $\mathcal{M}_h \subset \mathcal{M}$ is the discrete space of the Lagrange multiplier defined as the interpolation functions of compact support corresponding to the Lagrange polynomial restricted to the boundary. In the proposed model problem each domain may have non-matching domain triangulations see figure 2, furthermore the Lagrange multiplier will inherit the 1D discretization of the non-mortar side see figure 3.

5 NUMERICAL RESULTS

In this section the $h-$convergence of the primal variable and the Lagrange multiplier of the method is tested by solving an interface problem in a given domain. In addition the cell polarization process is numerically solved for the isolated system in figure 1 and for a cluster of cell. The active response of the cell membrane driven by the Hodgkin-Huxley model is also investigated for the idealized system.

5.1 h-convergence of the method

To evaluate the $h-$convergence of the mortar finite element method with Lagrange multiplier we solve numerically the follow second order elliptic problem on $\Omega = \Omega_1 \bigcup \Omega_2$, with $\Omega_2 = [-0.5, 0.5]^2$ and $\Omega_1 = [-1.0, 1.0]^2 \setminus \Omega_2$ as depicted in figure 4 left.

$$
\begin{aligned}
-\kappa_1 \Delta u_1 &= f_1, \quad \in \ \Omega_1 \\
-\kappa_2 \Delta u_2 &= f_2, \quad \in \ \Omega_2 \\
u_1 &= 0, \quad \text{on } \partial\Omega_1 \\
-\nabla u_1 \cdot \mathbf{n} &= -\nabla u_2 \cdot \mathbf{n}, \quad \text{on } \Gamma \\
u_1 - u_2 &= sin(\pi x) sin(\pi y), \quad \text{on } \Gamma
\end{aligned}
\tag{17}
$$

where $f_1 = f_2 = 4\pi^2 sin(\pi x) sin(\pi y)$, $\kappa_1 = 1$, $\kappa_2 = 2$ and the exact solution is given by,

$$
\begin{aligned}
u_1 &= 2sin(\pi x) sin(\pi y), \quad \in \ \Omega_1 \\
u_2 &= sin(\pi x) sin(\pi y), \quad \in \ \Omega_2.
\end{aligned}
\tag{18}
$$

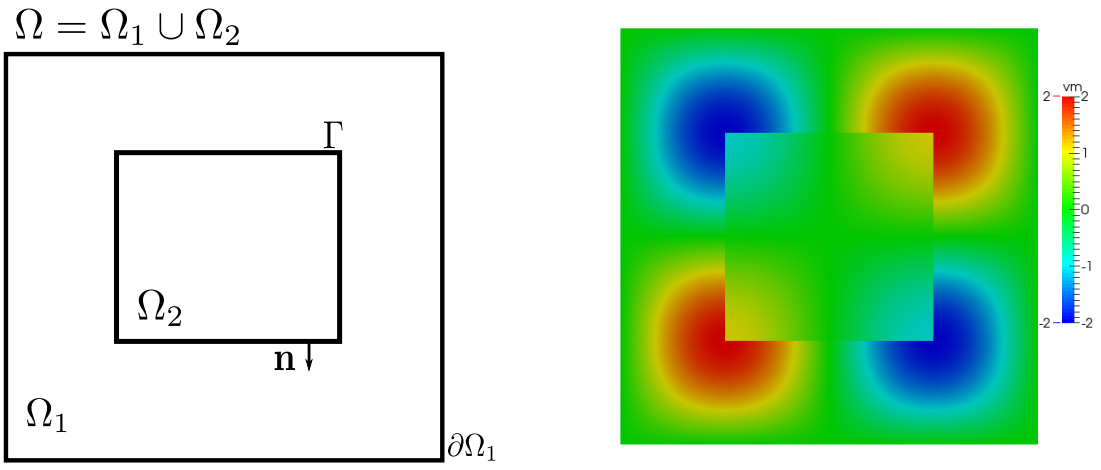

Figure 4: Computational domain and numerical solution of the second order interface problem.

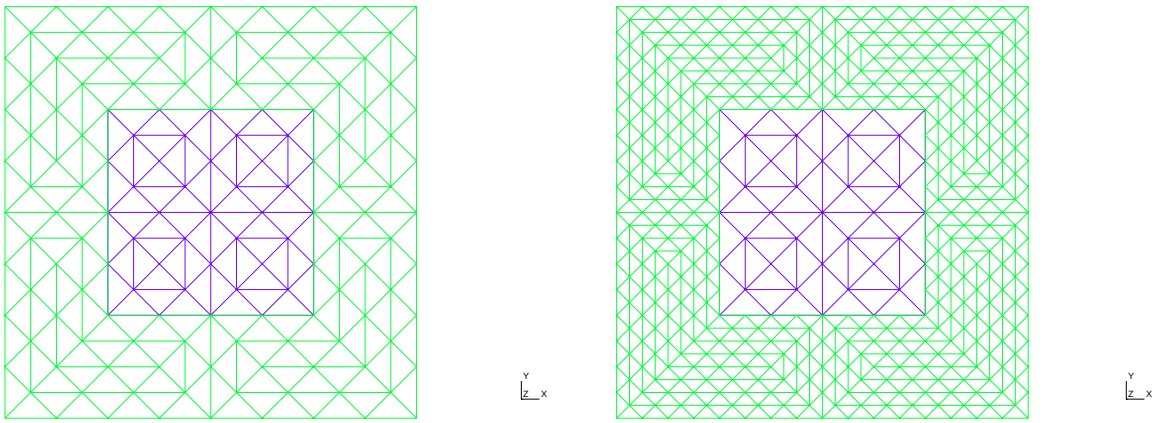

Figure 5: Domain discretization by triangular linear finite elements, matching discretization left and non-matching discretization at right.

The discrete primal hybrid variational formulation of problem 17 can be loosely written as

$$\begin{aligned} \kappa \int_{\Omega} \nabla u_h \cdot \nabla v_h dx + \int_{\Gamma} \lambda_h [v_h] ds &= \int_{\Omega} f v_h dx, \quad \forall v_h \in \mathcal{X}_h \\ -\int_{\Gamma} \mu_h [u_h] ds &= \int_{\Gamma} \mu_h sin(\pi x) sin(\pi y) ds, \qquad \forall \mu_h \in \mathcal{M}_h \\ u_1 &= 0, \quad \text{on } \Gamma_D \end{aligned} \tag{19}$$

with $\kappa = (\kappa_1, \kappa_2)$, $\Omega = \Omega_1 \bigcup \Omega_2$ and $f = (f_1, f_2)$. The $h-$convergence of the MFEM, in L^2 norm is tested for a domain discretization with triangular linear finite elements with matching and non-matching discretizations as shown in figure 5. In Table 1 and 2, are listed the the error in L^2 norm for the primal variable and the Lagrange multiplier for both cases.

	$\|u - u_h\|_{L^2(\Omega)}$		$\|\lambda - \lambda_h\|_{L^2(\Omega)}$	
mesh	**error**	**order**	**error**	**order**
16	1.12e-1	–	6.13e-1	–
32	3.48e-2	1.68	3.99e-1	0.62
64	9.24e-3	1.79	1.70e-1	0.93
128	2.36e-3	1.86	7.80e-2	1.02
256	5.96e-4	1.90	2.59e-2	1.15

Table 1: $h-$convergence order for the approximation of u_h and λ_h obtained by the MFEM for matching triangular elements.

In figure 6 the $h-$convergence curves of the MFEM for matching (left) and non-matching (right) discretizations is depicted.

$\|u - u_h\|_{L^2(\Omega)}$			$\|\lambda - \lambda_h\|_{L^2(\Omega)}$	
mesh	**error**	**order**	**error**	**order**
24	6.79e-2	–	4.87e-1	–
48	2.23e-2	1.61	3.66e-1	0.89
96	6.20e-3	1.73	2.12e-1	1.05
192	1.61e-3	1.80	1.11e-1	1.09

Table 2: $h-$convergence order for the approximation of u_h and λ_h obtained by the MFEM for non-matching triangular elements.

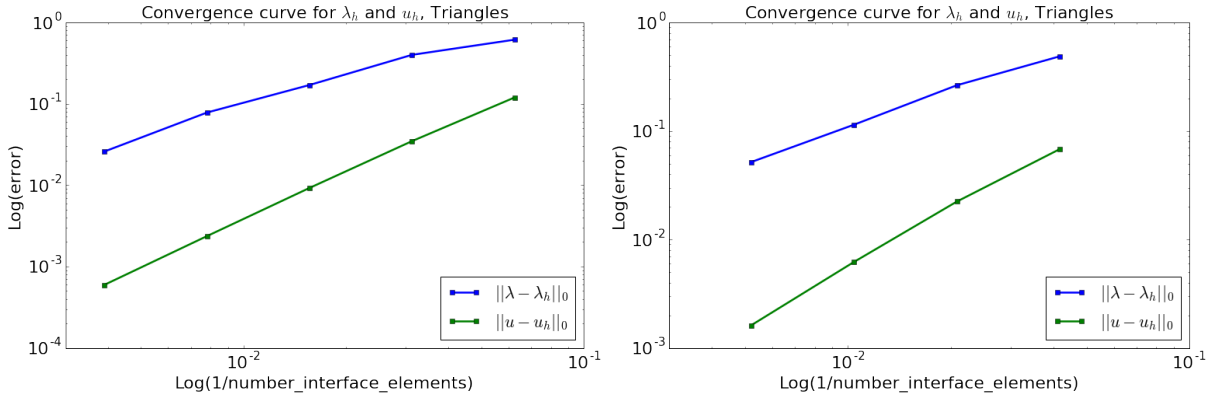

Figure 6: Convergence curve for the primal variable and the Lagrange multiplier for a triangular discretization with matching elements (left) and non-matching elements (right).

As noted from the $h-$convergence test, the mortar finite element method with Lagrange multiplier to impose the interface condition, converge with optimal $k+1$ rate for the primal variable u_h and with optimal rate k for the Lagrange multiplier λ_h, where k is the degree of the Lagrange polynomial base of approximation for triangular elements. In the next section the cell polarization and the active response of the cell membrane is investigated with the MFEM with Lagrange multiplier.

5.2 Cell polarization and active response of the cell membrane

For a simplified circular cell system as shown in figure 1, with an idealized ion current given by $I_{ion} = \frac{V_m}{R_m}$, the passive response of the cell can be solve in exact form, see (Ying & Henriquez, 2007). Here the exact and numerical solution of the electric potential distribution inside and outside the cell (u_i, u_e) at the membrane (fixed r) are plotted for different angular positions (θ), see figure 8, the reference system is shown in figure 7.

The cell polarization process takes place at time scale of microseconds, for an active response of the cell membrane proper of axioms and biological cell of the nervous system, the representative time scale is in milliseconds. The active response of the cell to an applied electric field can be investigate with the MFEM, in these case the $I_{ion}(V_m, \mathbf{q})$ of Eq. (14) is non-linear and is described by the Hodgkin-Huxley model, see (Hodgkin & Huxley, 1952). The time evolution

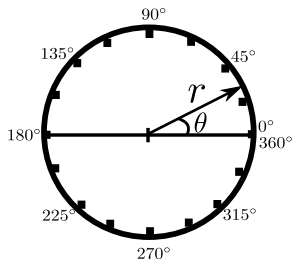

Figure 7: Reference system of the circular cell to plot the numerical and exact solution.

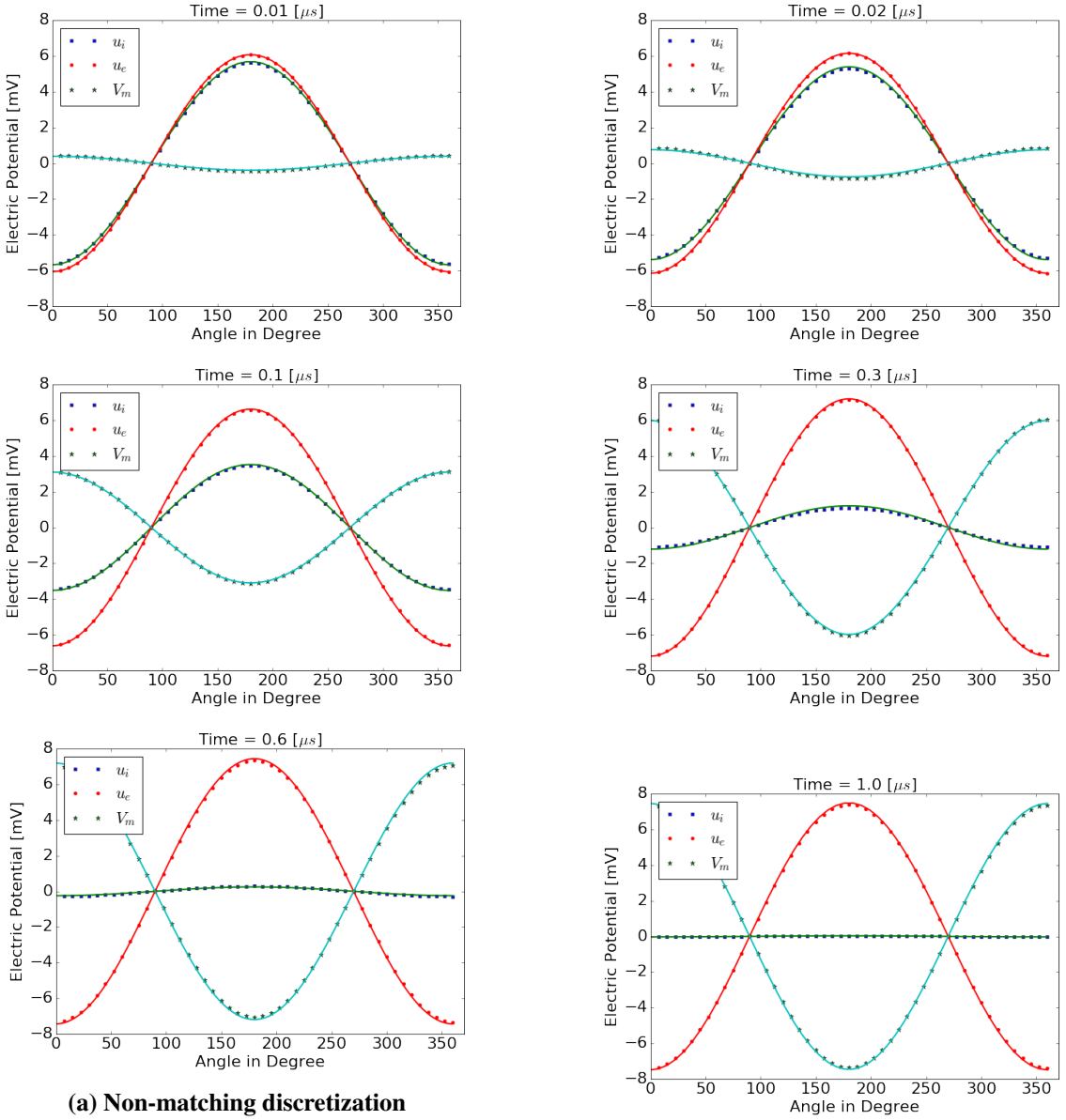

(a) Non-matching discretization

Figure 8: Electric potential in function of the angle evaluated at the membrane for the passive response of the cell. Exact solution is plotted as continuous functions, and the numeric result are point marker. Cell diameter $d_c = 15[\mu m]$, the intra and extracellular electric conductivity are $\kappa_i = 5[\mathrm{mS}\cdot\mathrm{cm}^{-1}]$ and $\kappa_e = 20[\mathrm{mS}\cdot\mathrm{cm}^{-1}]$, the membrane capacitance is $C_m = 1[\mu\mathrm{F}\cdot\mathrm{cm}^{-2}]$, the membrane resistance is $R_m = 1\mathrm{K}\Omega\cdot\mathrm{cm}^2$ and the applied electrical field is $\mathbf{E} = 5\mathrm{V}\cdot\mathrm{cm}^{-1}$.

of the electric potential inside and outside the cell for the active response of the cell for different angular positions, is plotted in figure 9.

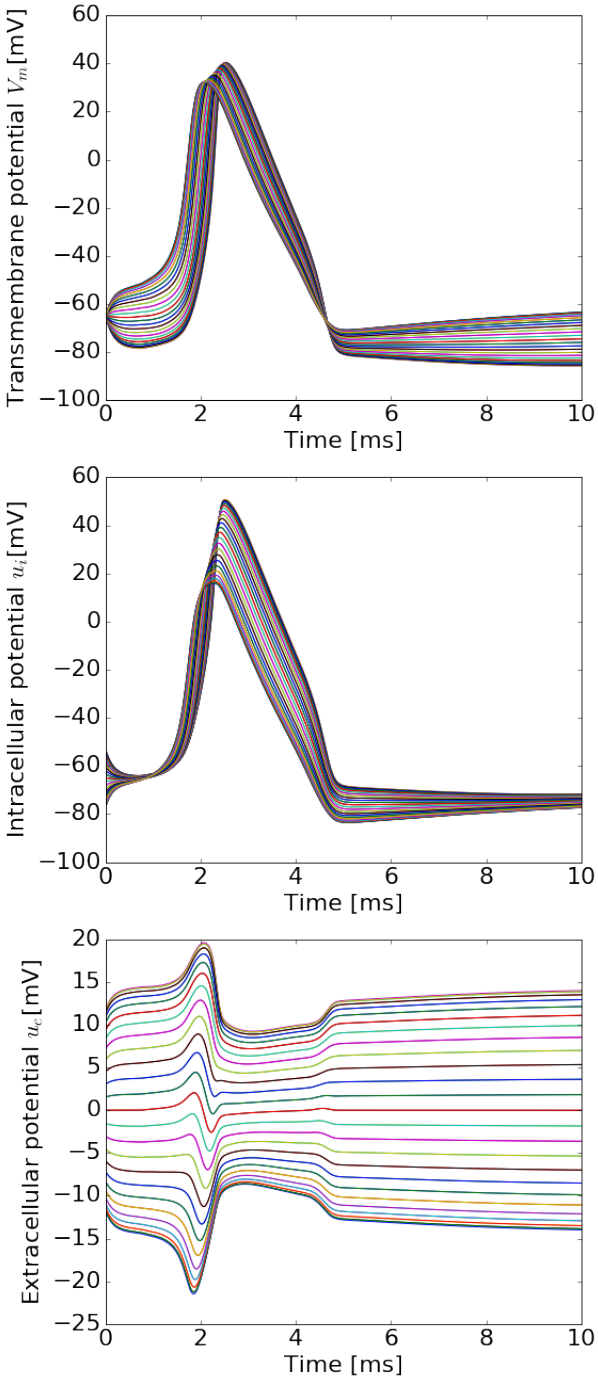

Figure 9: Active response of the cell to an applied electric field. Each curve follow the time course of the intracellular and extracellular electric potential for a fixed angle θ at the membrane (fixed r).

Note that the active response of the cell follow the typical curve of action potential described by the Hodgkin-Huxley model, physical quantities of electric conductivity inside and outside the cell were the same as in the passive response, in order to trigged action potential following the Hodgkin-Huxley model, the applied electric filed was $\mathbf{E} = 10[\mathrm{V} \cdot \mathrm{cm}^{-1}]$.

5.3 Spatial distribution of electric field in a cluster of cell

Understanding the distribution of electric potential in a conductive medium in the presence of biological cells is important to understand the influence of applied electrical field in neurons activity (Agudelo-Toro & Neef, 2013, Ying *et al.*, 2006), and on the study of drugs supply into the cell's cytosol trough electroporation (Chen *et al.*, 2006). With the presented numerical method the distribution of electric potential of a polarized cluster of cell is numerically investigated, see figures 10 and 11.

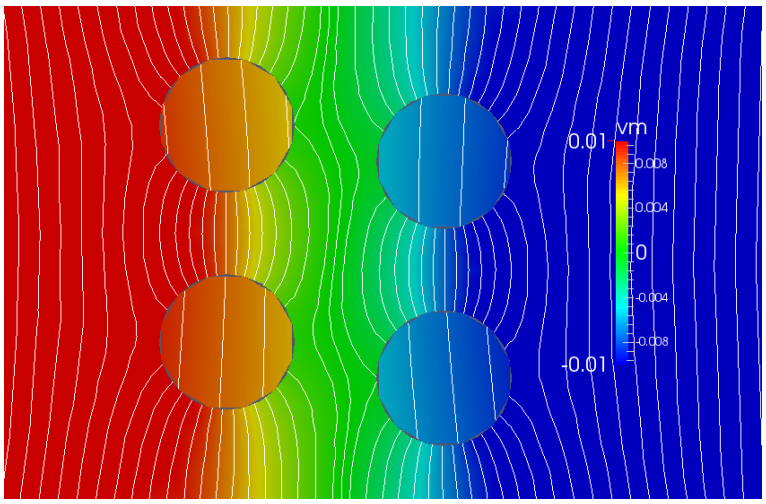

Figure 10: Iso-contour of electric potential in a passive response of a cluster of cell. Cell diameter $d_c = 15[\mu m]$, the intra and extracellular electric conductivity are $\kappa_i = 5[\text{mS} \cdot \text{cm}^{-1}]$ and $\kappa_e = 20[\text{mS} \cdot \text{cm}^{-1}]$, the membrane capacitance is $C_m = 1[\mu\text{F} \cdot \text{cm}^{-2}]$, the membrane resistance is $R_m = 1\text{K}\Omega \cdot \text{cm}^2$, the applied electrical field is $\mathbf{E} = 10\text{V} \cdot \text{cm}^{-1}$ and the distance between electrodes is $0.02[\text{cm}]$

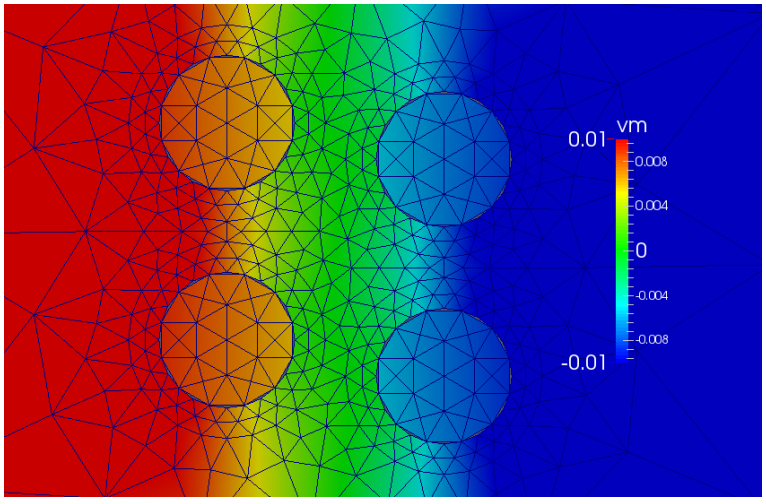

Figure 11: Non-matching discretization and electric potential magnitude in a cluster of cell.

6 FINAL REMARKS AND CONCLUSSIONS

The presented mortar finite element method with Lagrange multiplier for the cell interface problem, demonstrated to be an efficient tool to decoupled the non-linear problem of the active response of the cell from the boundary value problem of spatial distribution of electric potential. As demonstrated the numerical method can be effectively used to investigated the complex dynamics of the ionic current on the cell interface with a fully spatial representation of the distribution of the electric potential in a conductive medium in the presence of an arbitrary cell distribution.

The numerical method preserve the $h-$convergence property of the conforming finite element method, with the additional advantage of allowing non-matching domains discretizations.

ACKNOWLEDGEMENTS

The authors would like to thank to FAPEMIG, CAPES, CNPq and UFJF for the financial support during the development of this work.

REFERENCES

Agudelo-Toro, A. & Neef, A., 2013. Computationally efficient simulation of electrical activity at cell membranes interacting with self-generated and externally imposed electric fields. *Journal of Neural Engineering*. vol. 10, n. 2, p. 026019.

ASHIHARA, T., YAO, T., NAMBA, T., ITO, M., IKEDA, T., KAWASE, A., TODA, S., SUZUKI, T., INAGAKI, M., SUGIMACHI, M., KINOSHITA, M., & NAKAZAWA, K., 2001. Electroporation in a Model of Cardiac Defibrillation. *Journal of Cardiovascular Electrophysiology*. vol. 12, n. 12, pp. 1393–1403.

Belgacem, F. B., 1999. The Mortar finite element method with Lagrange multipliers. *Numerische Mathematik*. vol. 84, n. 2, pp. 173–197.

Benzi, M., Golub, G. H., & Liesen, J., 2005. Numerical solution of saddle point problems. *Acta numerica*. vol. 14, pp. 1–137.

Bernardi, C., Maday, Y., & Patera, A. T., 1993. *Domain Decomposition by the Mortar Element Method*. Springer Netherlands, Dordrecht. pp. 269–286.

Chen, C., Smye, S., Robinson, M., & Evans, J., 2006. Membrane electroporation theories: a review. *Medical and Biological Engineering and Computing*. vol. 44, n. 1, pp. 5–14.

Ciarlet, P., Kesavan, S., Ranjan, A., & Vanninathan, M., 1975. *Lectures on the Finite Element Method*. Lectures on mathematics and physics: Mathematics. Tata Institute of Fundamental Research.

Gimsa, J. & Wachner, D., 2001. Analytical description of the transmembrane voltage induced on arbitrarily oriented ellipsoidal and cylindrical cells. *Biophysical Journal*. vol. 81, n. 4, pp. 1888–1896.

Hodgkin, A. L. & Huxley, A. F., 1952. A quantitative description of membrane current and its application to conduction and excitation in nerve. *The Journal of Physiology*. vol. 117, n. 4, pp. 500–544.

Keener, J. & Sneyd, J., 2010. *Mathematical physiology: I: cellular physiology*. Springer Science & Business Media.

KRASSOWSKA, W., 1995. Effects of Electroporation on Transmembrane Potential Induced by Defibrillation Shocks. *Pacing and Clinical Electrophysiology*. vol. 18, n. 9, pp. 1644–1660.

Krassowska, W. & Neu, J., 1994. Response of a single cell to an external electric field. *Biophysical Journal*. vol. 66, n. 6, pp. 1768 – 1776.

Lamichhane, B. P., 2006. Higher order mortar finite elements with dual Lagrange multiplier spaces and applications.

Lee, D. C. & Grill, W. M., 2005. Polarization of a Spherical Cell in a Nonuniform Extracellular Electric Field. *Annals of Biomedical Engineering*. vol. 33, n. 5, pp. 603–615.

Nikolski, V. P. & Efimov, I. R., 2005. Electroporation of the heart. *EP Europace*. vol. 7, n. s2, p. S146.

Orlowski, S. & Mir, L. M., 1993. Cell electropermeabilization: a new tool for biochemical and pharmacological studies. *Biochimica et Biophysica Acta (BBA)-Reviews on Biomembranes*. vol. 1154, n. 1, pp. 51–63.

Plonsey, R. & Heppner, D. B., 1967. Considerations of quasi-stationarity in electrophysiological systems. *The bulletin of mathematical biophysics*. vol. 29, n. 4, pp. 657–664.

Pucihar, G., Miklavcic, D., & Kotnik, T., 2009. A time-dependent numerical model of transmembrane voltage inducement and electroporation of irregularly shaped cells. *IEEE Transactions on Biomedical Engineering*. vol. 56, n. 5, pp. 1491–1501.

Raviart, P.-A. & Thomas, J., 1977. Primal hybrid finite element methods for 2nd order elliptic equations. *Mathematics of computation*. vol. 31, n. 138, pp. 391–413.

Raviart, P.-A., Thomas, J.-M., Ciarlet, P. G., & Lions, J. L., 1998. *Introduction à l'analyse numérique des équations aux dérivées partielles*. vol. 2. Dunod Paris.

Šemrov, D. & Miklavčič, D., 2000. *Numerical Modeling for In Vivo Electroporation*. Humana Press, Totowa, NJ. pp. 63–81.

Susil, R., Šemrov, D., & Miklavčič, D., 1998. Electric Field-Induced Transmembrane Potential Depends on Cell Density and Organizatio. *Electro-and magnetobiology*. vol. 17, n. 3, pp. 391–399.

Valič, B., Golzio, M., Pavlin, M., Schatz, A., Faurie, C., Gabriel, B., Teissié, J., Rols, M.-P., & Miklavčič, D., 2003. Effect of electric field induced transmembrane potential on spheroidal cells: theory and experiment. *European Biophysics Journal*. vol. 32, n. 6, pp. 519–528.

Wohlmuth, B. I., 2000. A Mortar Finite Element Method Using Dual Spaces for the Lagrange Multiplier. *SIAM Journal on Numerical Analysis*. vol. 38, n. 3, pp. 989–1012.

Ying, W. & Henriquez, C. S., 2007. Hybrid finite element method for describing the electrical response of biological cells to applied fields. *IEEE Transactions on Biomedical Engineering*. vol. 54, n. 4, pp. 611–620.

Ying, W., Pourtaheri, N., & Henriquez, C. S., 2006. Field stimulation of cells in suspension: use of a hybrid finite element method. In *Engineering in Medicine and Biology Society, 2006. EMBS'06. 28th Annual International Conference of the IEEE*. IEEE. pp. 2276–2279.